

Enhancing the dielectric, electrocaloric and energy storage properties of lead-free $\text{Ba}_{0.85}\text{Ca}_{0.15}\text{Zr}_{0.1}\text{Ti}_{0.9}\text{O}_3$ ceramics prepared via sol-gel process

H. Mezzourh^{1,2}, S. Belkhadir¹, D. Mezzane¹, M. Amjoud¹, E. Choukri¹, A. Lahmar², Y. Gagou², Z. Kutnjak³, M. El Marssi²

¹ IMED, Cadi-Ayyad University, Faculty of Sciences and Technology, BP 549, Marrakech, Morocco.

² Laboratory of Physics of Condensed Matter (LPMC), University of Picardie Jules Verne, Scientific Pole, 33 rue Saint-Leu, 80039 Amiens Cedex 1, France.

³ Jozef Stefan Institute, Jamova Cesta 39, 1000 Ljubljana, Slovenia

Abstract

The $\text{Ba}_{0.85}\text{Ca}_{0.15}\text{Zr}_{0.1}\text{Ti}_{0.9}\text{O}_3$ (BCZT) ceramics were successfully prepared by sol-gel process, and sintered at 1420°C. The effect of sintering times (2, 4 and 6 h) on structural, microstructural, electric properties, energy storage, and electrocaloric effect was systematically examined. X-ray diffraction (XRD) results show that all the samples crystallize in the pure perovskite structure. The morphotropic phase transition from the tetragonal to the orthorhombic phase (T-O) was identified and confirmed by Rietveld refinement. The BCZT ceramic sintered at 1420°C for 4h possesses a good relative density of 98%, and exhibits optimal properties with a high dielectric permittivity ($\epsilon_{r,\text{max}}$) ~16310, a large electrocaloric effect coefficient (ξ) ~ 0.244Kmm/kV and an energy density storage of ~ 10.61 mJ/cm³.

Keywords : BCZT ceramics; sol-gel method; dielectric; electrocaloric effect; energy storage.

1. Introduction

Since many years, lead-based piezoelectric materials such as lead zirconium titanate PbTiO_3 – PbZrO_3 (PZT) [1], $\text{Pb}(\text{MgNb})\text{O}_3$ – PbTiO_3 (PMN-PT), and $\text{Pb}(\text{Ni}_{1/3}\text{Nb}_{2/3})\text{O}_3$ – PbHfO_3 – PbTiO_3 (PNN–PHT) [2] are extensively used in various functional applications such as non-volatile memory, sensors, actuators, transducers, capacitors, generators and energy harvesting devices, [3]–[6] due to their eminent electrical performance close to the morphotropic phase boundaries. However, these compounds have the undeniable disadvantage of toxicity and volatility of lead. The use of these materials has contributed in a serious environmental and human health problems [7], [8]. Recently, many scientific teams have been searching for new eco-friendly

alternative materials with advanced properties. By investigating various lead-free materials with perovskite structure (ABO_3) such as $BaTiO_3$ (BT), $(Bi_{0.5}Na_{0.5})TiO_3$ - $BaTiO_3$ (BNT-BT), $(K_{0.5}Na_{0.5})NbO_3$ (KNN) and $Ba_{1-x}Ca_xTi_{1-y}Zr_yO_3$ (BCZT) [9]–[11]. Among of all the above materials, barium calcium zirconate titanate ($(Ba,Ca)(Zr,Ti)O_3$, BCZT) exhibits a super large piezoelectric coefficient (d_{33}) up to 620 pC/N [12] in a bulk ceramic with perovskite structure, and possesses a high dielectric permittivity value of ~ 17184 [13] as well as important ferroelectric properties and low loss tangent ($\tan \delta$). It is thought that the high-performance of BCZT ceramics may stem from the morphotropic phase boundary that is a region of specific interest for electroceramic materials [14]. It is well known that, the chemical and electrical properties of electroceramics depend strongly on the synthesis methods and preparation conditions. Several synthesis techniques were employed to prepare perovskite powders such as solid-state technique, hydro-solvothermal synthesis and sol-gel process [15]–[18]. Many papers have reported that the sol gel method provides a better homogeneity, chemical purity, and stoichiometric composition of the resultant phase comparing to the ceramics prepared by solid state method [19]. In general, the sintering factors such as temperature and dwelling time affect the structural and electrical properties of BCZT ceramics [20], [21]. Cai et al. reported that excellent ferroelectric properties ($2Pr = 31.62 \mu C/cm^2$, $2Ec = 3.46 kV/cm$) of $Ba_{0.85}Ca_{0.15}Zr_{0.1}Ti_{0.9}O_3$ ceramics obtained by sol-gel method, can be achieved by sintered at $1500^\circ C$ for 10h [22]. Moreover, an interesting recoverable energy density value of $0.52 J/cm^3$ reported in $Ba_{0.85}Ca_{0.15}Zr_{0.1}Ti_{0.9}O_3$ by Wang et al. [19] indicates that this ceramic could be a promising candidate for energy storage applications. On the other hand, Rui Liu et al. found that the ceramic sintered at $1420^\circ C$ exhibits a good dielectric permittivity with a weak dielectric loss ~ 0.015 [23], [24]. In that regard, our group has reported that BCZT-spherical nanoparticles and BCZT-rod like ceramics elaborated by surfactant-assisted solvothermal route exhibit enhanced dielectric, ferroelectric and electrocaloric properties [25]. In addition, we have studied the influence of the sintering temperature on the microstructure, dielectric and diffusivity of the BCZT ceramic prepared by sol-gel method [26]. In the present work, we investigate the effect of sintering dwell time at $1420^\circ C$ on the dielectric, electrocaloric and energy storage properties of BCZT ceramics prepared by sol-gel technique.

2. Experimental details

2.1. Chemicals

For the preparation of BCZT ceramics, the following materials purchased from Sigma-Aldrich and Alfa Aesar, were used: barium acetate $\text{Ba}(\text{CH}_3\text{COO})_2$, calcium nitrate tetrahydrate $\text{Ca}(\text{NO}_3)_2 \cdot 4\text{H}_2\text{O}$, titanium (IV) isopropoxide $\text{Ti}[\text{OCH}(\text{CH}_3)_2]_4$ and zirconium (IV) oxychloride octahydrate $\text{ZrOCl}_2 \cdot 8\text{H}_2\text{O}$ as the starting materials, acetic acid and 2-Methoxyethanol were used as the solvents.

2.2. Synthesis procedure

The $\text{Ba}_{0.85}\text{Ca}_{0.15}\text{Zr}_{0.1}\text{Ti}_{0.9}\text{O}_3$ (BCZT) ceramic was synthesized by sol-gel route. Firstly, the $\text{Ba}(\text{CH}_3\text{COO})_2$ and $\text{Ca}(\text{NO}_3)_2 \cdot 4\text{H}_2\text{O}$ were initially dissolved completely in acetic acid according to the stoichiometric ratio under continuous stirring. Afterward, stoichiometric amount of $\text{ZrOCl}_2 \cdot 8\text{H}_2\text{O}$ was dissolved in 2-Methoxyethanol solution, then $\text{Ti}[\text{OCH}(\text{CH}_3)_2]_4$ was added and stirred. In the next step, this solution was added to above (Ba, Ca) precursor solution and stirred for 1h at room temperature to yield a clear transparent BCZT solution. The pH was adjusted with ammonia to 6. The obtained sol was dried at 120°C for 24 h to eliminate the solvents, and then grounded to fine powder in a mortar. The powder was calcined for 4 h at 1000°C in air to form a pure crystalline phase. Then, the calcined powder was pressed into cylindrical disks with a diameter of 13 mm by uniaxial pressing under 100 MPa. Finally, the samples were sintered at 1420°C in air atmosphere for 2, 4 and 6h and designated BCZT-t, where t is the sintering dwell time.

2.3. Characterization equipments

The phase structure of the sintered ceramics was determined by X-ray diffraction (XRD, Panalytical X-Pert Pro) analysis using the $\text{Cu-K}\alpha$ radiation with $\lambda \sim 1.540598 \text{ \AA}$. The measurements were performed at room temperature in a range from 20° to 80° with the step size of 0.02° . Rietveld refinement analysis was achieved by using FullProf software.

The morphologies of the surfaces were revealed by a Scanning Electron Microscope (SEM, VEGA 3-Tscan) in association with energy dispersive X-ray (EDX) analysis. The densities of the pellets were measured using the Archimedes method [11]. The dielectric measurements and

the impedance spectroscopy were examined by using an HP 4284A precision impedance meter, controlled by a computer in the 20Hz to 1MHz frequency range. The sintered samples surfaces were covered with a conductive silver paste serving as electrodes for electrical measurements. The polarization-electric field (P-E) hysteresis loops were collected using a commercial ferroelectric test system (TF Analyzer 3000, aixACCT). The electrocaloric adiabatic temperature variation (ΔT) and responsivity (ζ) were achieved by the indirect method from recorded (P-E) hysteresis loops at 1 Hz as a function of temperature.

3. Results and discussion

3.1. Structural analysis : XRD

Figure.1 presents the X-ray diffraction patterns of BCZT ceramics sintered for various dwell times. All samples exhibit pure perovskite structure without any secondary phase in the limite of device detection, suggesting that Ca^{2+} and Zr^{4+} have diffused into the BaTiO_3 lattice to form a solid solution [27]. The Rietveld refinement of all ceramics shows the coexistence of tetragonal, T (space group P4mm) and orthorhombic, O (space group Amm2) phase at room temperature [28], [29]. Structural information and phase composition are enlisted in **Table. 1**. The crystallite size was determined using Scherrer's formula [30] as following :

$$D = \frac{k \times \lambda}{\beta \times \cos\theta} \quad (1)$$

Where, k is the Scherrer constant, λ is the wavelength of the X-Rays used for the diffraction, β the « full width at half maximum » of the sharp peaks, and θ is the measured angle. From the **Table. 1**, it is observed that the crystallite size increases with increasing the dwell time, indicating better crystallinity for longer sintering time [31].

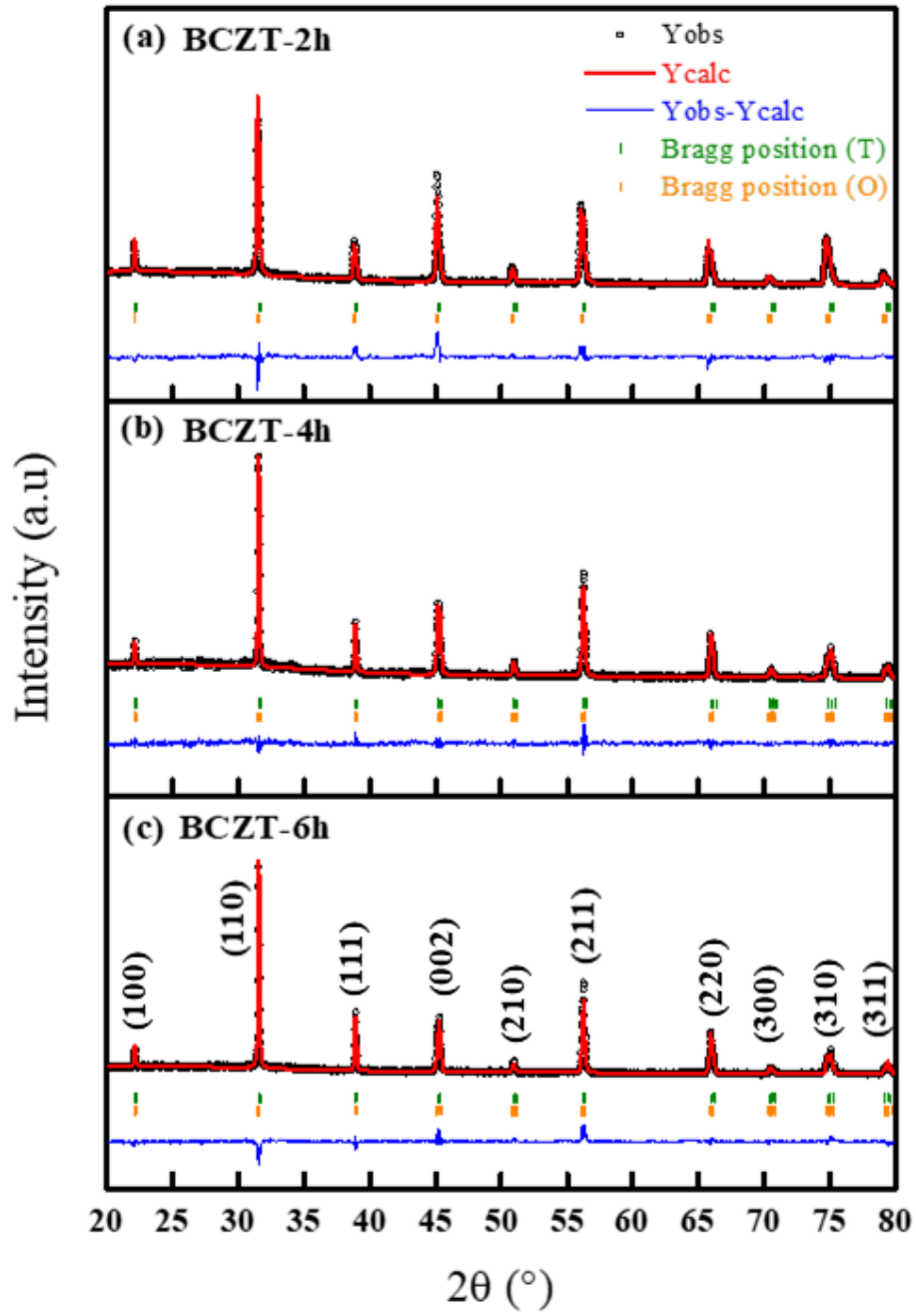


Fig.1. XRD patterns and Rietveld refinement of BCZT samples sintered for various dwell times : (a) 2h, (b) 4h and (c) 6h.

Table. 1. Structural parameters, average crystalline size, average grain size and relative density of BCZT ceramics sintered at different dwell times.

Sintering time (h)	Structure	Unit cell parameters				Tetragonality (c/a)	Phase compositions (wt%)	Reliability factors (%)			Average crystalline size (nm) by XRD	Average grain size(μm) by SEM	Relative density (%)
		a(\AA)	b(\AA)	c(\AA)	V (\AA^3)			Rwp	Rp	χ^2			
2	Tetragonal	3.9989	3.9989	4.0053	64.052	1.0016	55.92	24.3	33.8	0.88	24.96	28.04	94.5
	+ Orthorhombic	4.0188	4.0130	4.0144	64.744								
4	Tetragonal	3.9928	3.9928	4.0092	63.918	1.0041	77.52	27.8	42.5	1.06	32.95	30.79	98.5
	+ Orthorhombic	3.9957	4.0134	4.0053	64.231								
6	Tetragonal	3.9988	3.9988	4.0122	64.159	1.0033	60.60	27.6	35.7	0.94	27.84	33.23	97.8
	+ Orthorhombic	4.0162	3.9952	4.0073	64.300								

3.2. Microstructural and compositional analyses

Figure. 2 displays the SEM images of the surface morphologies of the sintered BCZT ceramics with different sintering times of 2, 4 and 6h (insets show the corresponding histograms). It can be clearly seen that all the BCZT ceramics are densely sintered with irregular shaped and large grains up to micrometers. Furthermore, as shown in **Figure. 2a-c**. The average grain size estimated using an analytical software (image J) has increased from 28 to 33 μm with increasing sintering time from 2h to 6h. The relative density of all studied samples is greater than 94 %, this could be attributed to the highly active and well dispersion precursor powder prepared by the sol gel method [32]. Furthermore, it could be suggested that the sintering temperature of 1420°C was sufficient for the BCZT powder to produce good quality ceramics. The relevant grain size distributions and relative densities estimated are listed in **Table. 1**.

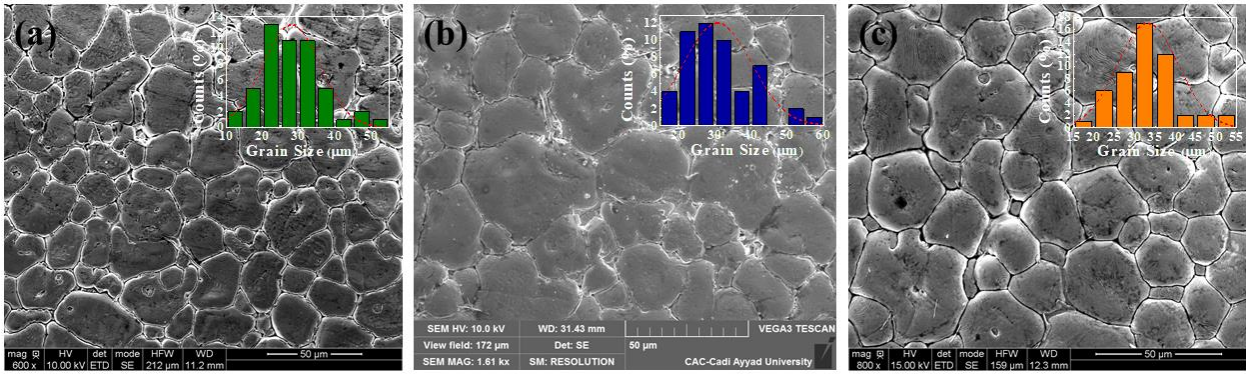


Fig.2. SEM micrographs and grain size distributions with Gaussian fitting (inset) of the samples sintered at various dwell times : (a) 2h, (b) 4h and (c) 6h.

To confirm the chemical composition of the BCZT ceramics, the ceramic elements distribution were performed by the EDX analysis, as presented in **Figure 3**, which indicates the presence of Ba, Ca, Ti, Zr and O elements. It also gives the ratios of Ba to Ca and Zr to Ti as 5.38 and 9.67 respectively, that confirms the as-prepared composition : as $\text{Ba}_{0.85}\text{Ca}_{0.15}\text{Zr}_{0.1}\text{Ti}_{0.9}\text{O}_3$. No other peak for any other element has been detected in the spectrum confirming the XRD observation and the chemical purity of the BCZT ceramics prepared by the sol-gel method.

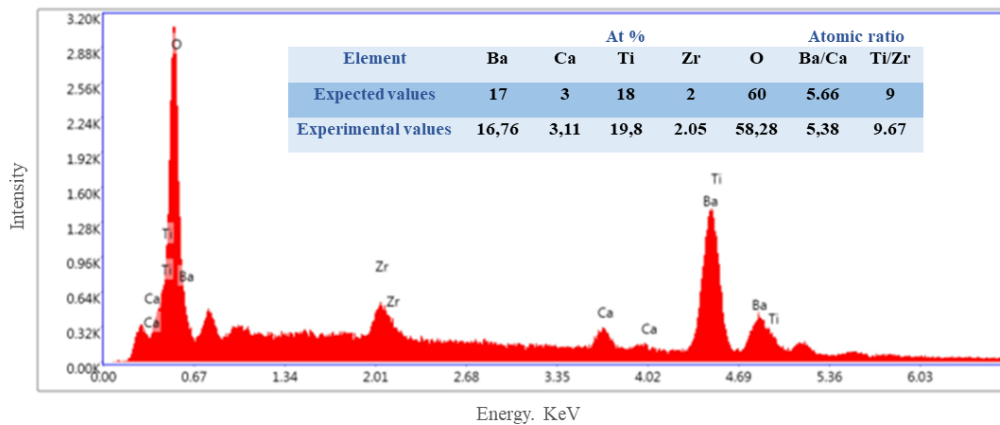


Fig.3. EDX spectra of BCZT ceramic sintered for 4h.

3.3. Dielectric analysis

The temperature dependence of the relative dielectric permittivity (ϵ_r) and dielectric loss factor ($\tan \delta$) of BCZT ceramics measured from room temperature to 200 °C are shown in **Figure 4**. Two dielectric anomalies were observed for all samples: the first one corresponds to the morphotropic phase transition from the orthorhombic to tetragonal (O-T) phase, with increasing

sintering time T_{O-T} shifts from 31 to 24°C, while T_c shifts to higher temperature with increasing sintering time. The exact origin of this behavior is still unclear. The coexistence of the two phase structures in these ceramics may lead to good electrical properties. The dielectric permittivity maximum ($\epsilon_{r,max}$) values depend greatly on sintering time as shown in **Table. 2**. It is worth noting that the BCZT-4h exhibits the largest value of dielectric permittivity ($\epsilon_{r,max} \approx 16310$, at 1 kHz), which is higher and/or similar to that obtained by other literature reported on BCZT ceramics prepared by different methods as illustrated in **Table. 3**. The significant improvement of the dielectric permittivity could be related to the high density of BCZT-4h [33]. All samples keep a low value of $\tan \delta$ (≤ 0.06 , at 1 kHz), this is probably attributed to the dense microstructure and the lower electron diffusion in the grain boundaries [34]. The overall properties (T_c , $\epsilon_{r,max}$, $\tan \delta_{T_c}$) are recorded and summarized in **Table. 2**.

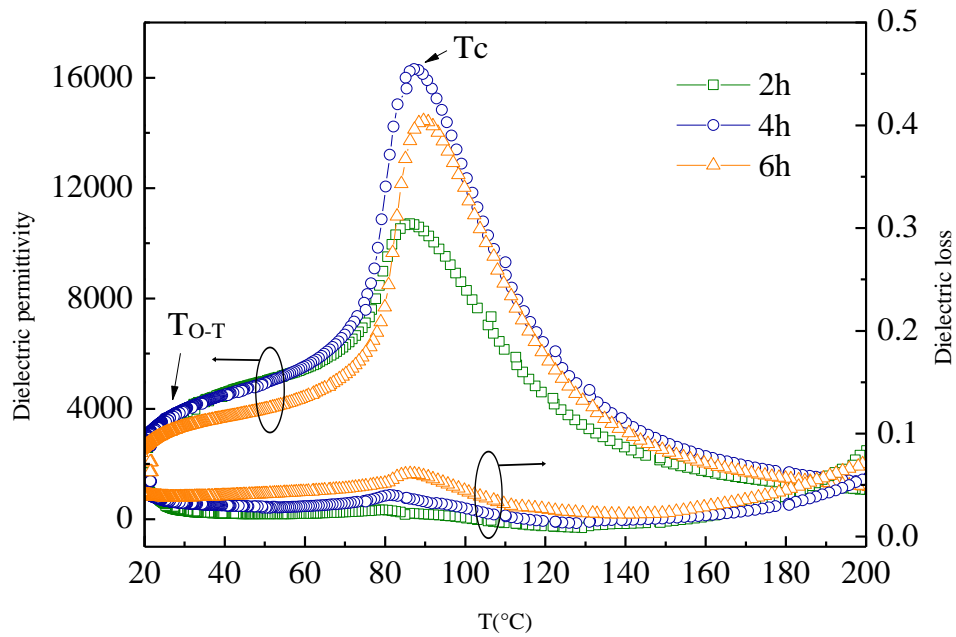


Fig.4. Variations of dielectric properties of BCZT samples sintered at various sintering times with the temperature measured at 1 kHz.

The temperature dependence of the dielectric permittivity for BCZT-4h ceramic at different frequencies, ranging from 100 Hz to 100 kHz is illustrated in **Figure. 5**. The first derivative of relative permittivity as a function of temperature is plotted (**inset of Figure. 5**). It is noticed that the dielectric maximum decreases as a function of frequency. This may be attributed to the decrease of the net polarization due to the accumulation of space charges at the grain boundaries

which subsequently leads to the formation of interfacial polarization. In general, as frequency increases, the net polarization decreases as each polarization mechanism ceases to contribute, and hence, its dielectric constant decreases [26], [35], however, there is no frequency dispersion in T_C . These two behaviors are associated with the diffuse phase transition in all samples and differs from the relaxor materials [36].

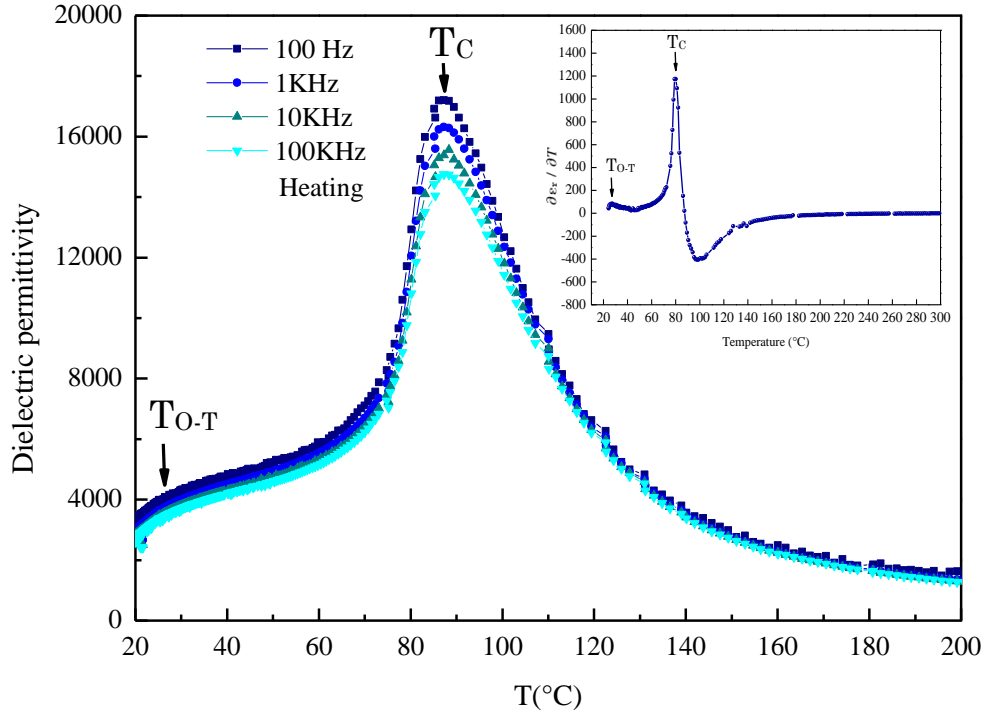


Fig.5. Temperature dependence of dielectric permittivity at different frequencies of BCZT samples sintered for 4h. Inset : Derivative of relative dielectric permittivity as a function of temperature.

It is known that the classical ferroelectrics follow the Curie-Weiss law above Curie temperature [37] which is defined by the following equation:

$$\frac{1}{\epsilon_r} = \frac{T - T_0}{C} \quad (T > T_0) \quad (2)$$

Where T_0 denotes the Curie–Weiss temperature and C is the Curie –Weiss constant reflecting the nature of the ferroelectrics transition.

The temperature-dependence of reciprocal dielectric permittivity at a frequency of 1kHz for BCZT-4h ceramic is presented in **Figure. 6**.

The values of the fitting results obtained by Eq. (2) are listed in the **Table. 2**. The Curie constant value for all samples is in the order of 10^5 K, which are accordant with that of typical displacive-type ferroelectric [38].

The changes of Curie–Weiss behavior (ΔT_m) indicate the deviation from the Curie–Weiss law and the degree of diffuseness [39], which can be defined by :

$$\Delta T_m = T_{cw} - T_m \quad (3)$$

where T_{cw} represents the temperature at which the dielectric permittivity begins to deviate from Curie-Weiss law, and T_m is the temperature at maximum dielectric permittivity.

It is found that ΔT_m values are 39.74, 40.89 and 39.93°C for sintering times of 2, 4 and 6h, respectively, which implies a weaker diffuse phase transition behavior [31].

To explain the diffuseness phase transition, a modified form of Curie-Weiss law [40], proposed by Uchino is used which is given as follows:

$$\frac{1}{\varepsilon_r} - \frac{1}{\varepsilon_m} = \frac{(T - T_m)^\gamma}{C} \quad (1 \leq \gamma \leq 2) \quad (4)$$

where ε_r is the relative permittivity, ε_m is the maximum relative permittivity, T_m is the temperature of the maximum dielectric permittivity, C is the Curie–Weiss constant and γ is the degree of diffuse phase transition, with $1 < \gamma < 2$, this parameter gives information about the character of phase transition ; $\gamma = 1$ corresponds to normal ferroelectrics and $\gamma = 2$ corresponds to relaxor ferroelectrics. The inset in **Figure. 6** illustrates the linear fit plots of $\ln(1/\varepsilon_r - 1/\varepsilon_m)$ versus $\ln(T - T_m)$ at 1kHz for BCZT-4h ceramic and the value of γ is obtained from of the fitting curves. The values of γ are 1.760, 1.792 and 1.783 for 2, 4 and 6h, respectively, which indicate an incomplete diffuse phase transition behavior [41].

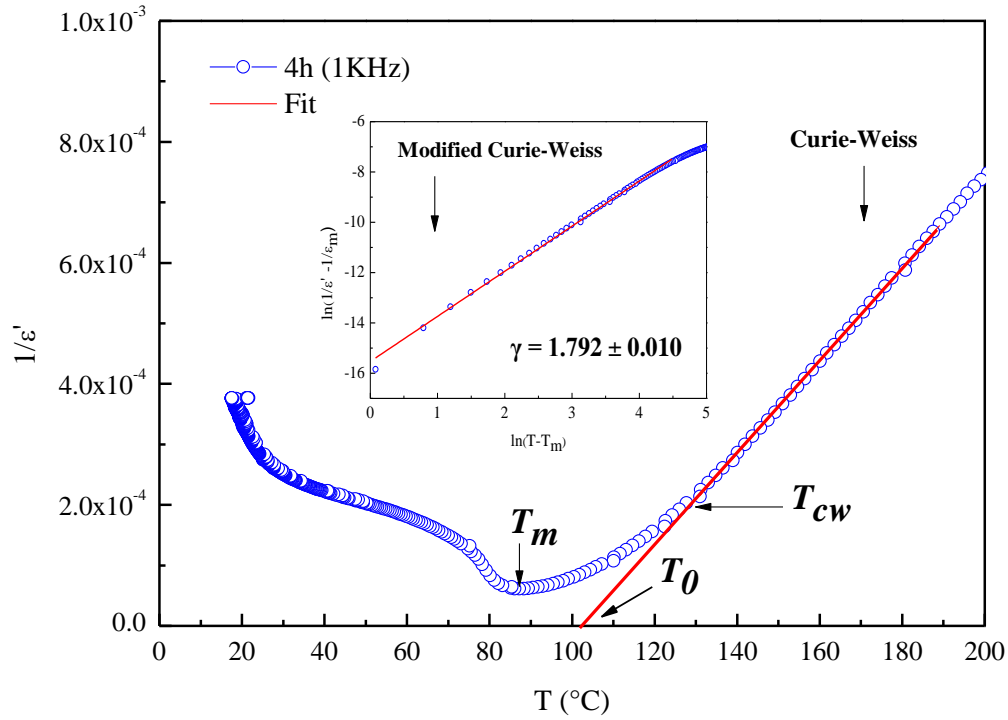


Fig.6. Curie–Weiss fitting curves of BCZT samples sintered for 4h.

Table. 2. Dielectric properties of BCZT ceramics performed at 1 kHz

Sintering time (h)	$\epsilon_{r,max}$ at 1kHz	$\tan\delta_{max}$ at 1kHz	T_{O-T} (°C)	T_m (°C)	T_0 (°C)	T_{cw} (°C)	ΔT_m (°C)	$C \times 10^5$ (°C)	γ
2	10704	0,025	31	86.20	98.67	125.94	39.74	1.052	1.760
4	16310	0,040	27	87.22	102.61	128.11	40.89	1.302	1.792
6	14439	0,060	24	89.60	104.39	129.53	39.93	1.118	1.783

3.4. Ferroelectric analysis

In order to assess the EC effect, P-E hysteresis loops were registered for the BCZT-4h ceramic at different temperatures as showed in **Figure. 7**. It can be seen from the hysteresis loops that the increase of temperature increases the ferroelectric properties which is the typical characteristic of ferroelectric to paraelectric phase transition.

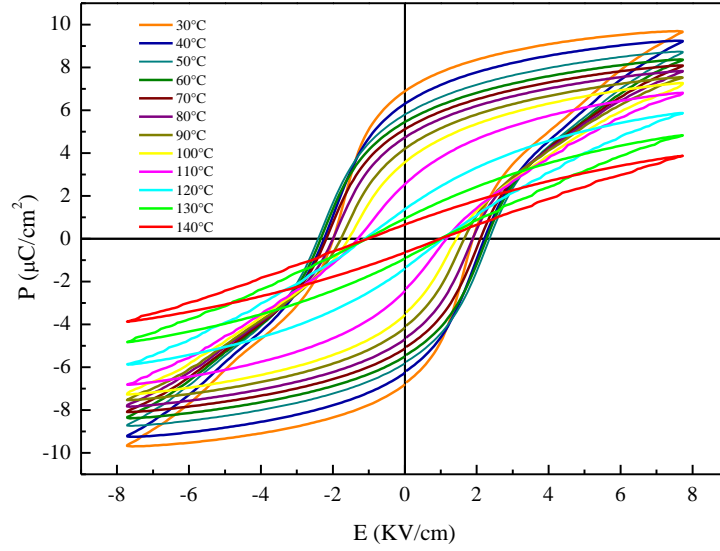


Fig. 7. P-E hysteresis loops of the BCZT samples sintered for 4h.

The grain size, density and phase homogeneity, affect the E_c , P_s , P_r and the squareness of the hysteresis loops. For an ideal hysteresis loop, the squareness parameter is equal to 2. According to Haertling and Zimmer, the squareness of the P-E loops can be quantitatively calculated using the following equation [42], [43] :

$$R_{sq} = \frac{P_r}{P_s} + \frac{P_{1.1E_c}}{P_r} \quad (5)$$

Where, R_{sq} is the squareness of hysteresis loop, P_s is saturation polarization, P_r is remnant polarization and $P_{1.1E_c}$ represents the polarization at an electric field equal to 1.1 times the coercive field (E_c). It can be seen that all samples exhibit approximately a value close to 2 (see **Table. 3**) indicating a better homogeneity and uniformity in grain size of the samples prepared by sol-gel which contribute to a fast domain switching [44].

Figure. 8 displays the comparative (P-E) loops of polarization versus electric field of the sintered BCZT ceramics with various dwell time of 2, 4 and 6 h measured at room temperature under critical electric field. It can be clearly seen that the sintering dwell time has a significant effect on the ferroelectric properties (E_c , P_s , P_r) of BCZT ceramics. Indeed, the E_c of BCZT ceramics decreases from 2.3131 to 1.7427 kV/cm with an increase of dwell time from 2h to 6h. These values are lower and/or nearly the same as observed in others BCZT ceramics prepared

by different processes and under various sintering conditions (see **Table. 3**). However, for BCZT-4h, P_s and P_r initially increase to a maximum values of 9.6955 and 6.8854 $\mu\text{C}/\text{cm}^2$ respectively and then decrease as showed in **Table. 3**. The great ferroelectric properties of BCZT-4h can be attributed to its high relative density (>98%) and large grain size (30.79 μm), it could be understood that the BCZT-4h possesses the critical grain size over which the electrical properties can be enhanced.

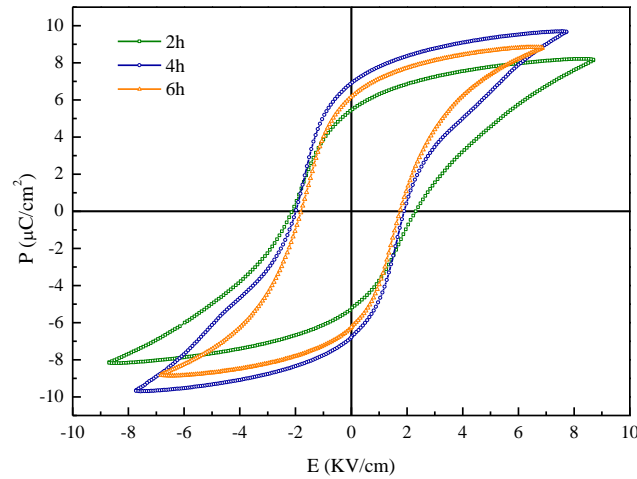


Fig. 8. Room-temperature P–E curves of the BCZT samples.

Table. 3. Comparison of dielectric and ferroelectric properties of BCZT ceramics in the present work with others reported in literature for various synthesis methods and sintering conditions.

Sintering regime (°C-h)	Synthesis method	Average grain size(μm)	Relative density (%)	$\epsilon_{r,\text{max}}$	$\tan\delta_{\text{max}}$	R_{sq}	P_s ($\mu\text{C}/\text{cm}^2$)	P_r ($\mu\text{C}/\text{cm}^2$)	E_c (kV/cm)	E (kV/cm)	Refs
1420-2	Sol-gel	28.04	94.5	10704	0,025	1.9653	8.2134	5.4410	2.3131	8.75	This work
1420-4	Sol-gel	30.79	98.5	16310	0,040	1.9295	9.6955	6.8854	1.8979	7.77	This work
1420-6	Sol-gel	33.23	97.8	14439	0,060	1.9424	8.8492	6.1749	1.7427	6.89	This work
1400-2	Sol-gel	---	95	8808	0.02	---	18	12.24	2.66	30	[45]
1420-6	Sol-gel	---	----	16480	0.015	---	17.76	11.64	1.78	30	[19]

1350-2	Sol-gel	1.5	---	6500	0.2	---	3	0.7	1.9	12	[46]
1400-2	Sol-gel- hydrothermal	---	95	9173	---	---	42	12.56	≈2.16	40	[31]
1300-3	Hydrothermal	12.09	---	7760	0.1	---	25	10.835	2.265	15	[39]
1500-4	Solid state	32.2	97.2	16300	0.017	---	24	12	5	55	[10]
1500-2	Solid state	20.8	---	9926	0.0108	---	---	---	---	---	[47]
1300-3	Solid state	27.61	95	4500	0.12	---	13.8	10.8	5.8	30	[48]

3.5. Energy storage performances

Generally, for nonlinear dielectrics, the recoverable energy density W_{rec} , total energy density W_{total} , and energy storage efficiency η can be determined from the polarization hysteresis (P-E) loops using the following equations [49]:

$$W_{total} = \int_0^{P_{max}} E dP \quad (6)$$

$$W_{rec} = \int_{P_r}^{P_{max}} E dP \quad (7)$$

and

$$\eta = \frac{W_{rec}}{W_{total}} \times 100 \quad (8)$$

Where P_{max} , P_r , E , W_{total} , W_{rec} and η refer to maximum polarization, remnant polarization, applied external electric field strength, energy storage density, recoverable energy density, energy storage efficiency respectively. **Figure. 10** shows the variation of W_{rec} , W_{loss} and η for BCZT ceramics as a function of sintering time. The BCZT-4h ceramic showed the better recoverable energy density (green area in **Figure. 9**) W_{rec} (10.61 mJ/cm³ at ~ 7.77 kV/cm), this improvement of W_{rec} may be due to the large P_s values and low E_c values, which facilitate the reorientation of dipoles with less electrical field. The values of efficiency (η) of the samples are relatively comparable with others previously reported in the literature under strong electric field

(see **Table. 4**). The best value of efficiency is $\eta=63.65\%$ at 140°C under an electric field of $\sim 7.77\text{ kV/cm}$, which is relatively comparable with others reported in the literature under strong electric field.

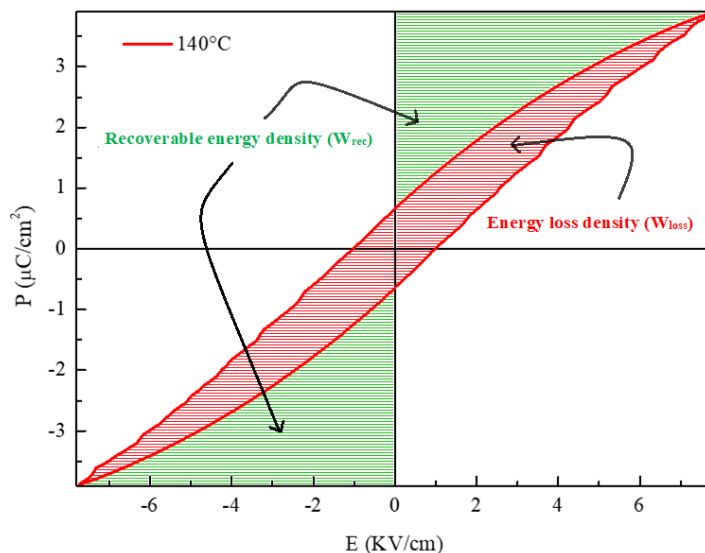


Fig. 9. P–E curve of the BCZT-4h at 140°C with schematic for the calculation of energy storage performance.

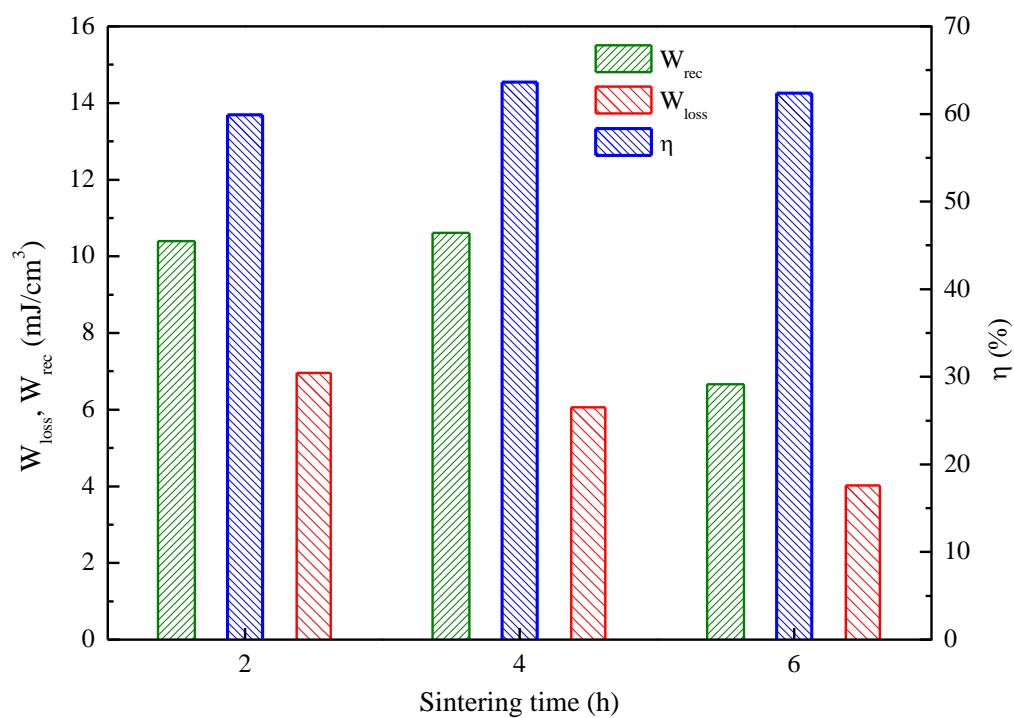


Fig. 10. Energy-storage properties of the BCZT samples with as a function of sintering time.

Table 4. Comparison of energy storage properties of the BCZT family ceramics.

Material	Sintering regime (°C-h)	Synthesis method	W_{rec} (mJ/cm ³)	W_{loss} (mJ/cm ³)	η (%)	E (kV/cm)	Refs
Ba _{0.85} Ca _{0.15} Zr _{0.1} Ti _{0.9} O ₃	1420-2	Sol-gel	10.40	6.96	59.90	8.75	This work
Ba _{0.85} Ca _{0.15} Zr _{0.1} Ti _{0.9} O ₃	1420-4	Sol-gel	10.61	6.06	63.65	7.77	This work
Ba _{0.85} Ca _{0.15} Zr _{0.1} Ti _{0.9} O ₃	1420-6	Sol-gel	6.66	4.02	62.36	6.89	This work
Ba _{0.85} Ca _{0.15} Zr _{0.1} Ti _{0.9} O ₃	1420-6	Sol-gel	520	---	---	30	[19]
Ba _{0.85} Ca _{0.15} Zr _{0.1} Ti _{0.9} O ₃	1420-6	Solid state	310	---	---	30	[19]
[(BaZr _{0.2} Ti _{0.80})O ₃] _{0.85} [(Ba _{0.70} Ca _{0.30})TiO ₃] _{0.15}	1600-4	Solid state	940	680	72	170	[50]
Ba _{0.85} Ca _{0.15} Zr _{0.1} Ti _{0.9} O ₃	1320-6	Co-precipitation	250	130	65	100	[51]
Ba _{0.95} Ca _{0.05} Zr _{0.3} Ti _{0.7} O ₃	1280-2	Citrate method	590	---	72.8	160	[52]

3.6. Indirect electrocaloric measurements

Using Maxwell relation $(\frac{\partial P}{\partial T})_E = (\frac{\partial S}{\partial E})_T$ the adiabatic temperature change ΔT under an applied electric field is calculated by the following equation [53]:

$$\Delta T = -\frac{1}{\rho} \int_{E_2}^{E_1} \frac{T}{C_p} (\frac{\partial P}{\partial T})_E dE \quad (9)$$

where ρ is the density of the ceramics, E_1 and E_2 are the lower and higher electric field limits, respectively, C_p denotes the specific heat capacity of the ceramics.

There are several factors that can influence the performance of the electrocaloric materials, the nature of the phase transition is one of these factors. Two types of transitions can be distinguished; first order transition is associated with a high value of ΔT with a restricted temperature range around T_c , while the second order transition is generally characterized by a low electrocaloric effect with a large temperature range around T_c [54].

The electrocaloric (EC) properties of the fabricated BCZT ceramics for an applied electric field 6 kV/cm are shown in **Figure 11**. The BCZT-4h and BCZT-6h present high values of $\Delta T_{\text{EC,max}}$

(0.1467K and 0.1513K respectively) in a limited temperature ranges, this may be related to the increase of the spontaneous polarization. This behavior indicates that the phase transition is of first order. However, BCZT-2h presents very low value of $\Delta T_{EC,max}$ with relatively large temperature range ($FWHM_{\Delta T}$) of $\approx 56K$, which indicates that the transition is of second order. The EC responsivity ($\xi=\Delta T/\Delta E$) values obtained for the BCZT samples are enlisted in **Table. 5**, comparing with different studies reported in literature. We notice that the BCZT ceramics sintered at 4h and 6h exhibit high EC responsivity of 0.244 K mm/kV and 0.252 K mm/kV respectively at low applied electric field of 6 kV/cm. These values appear to be comparable and/or higher than those of the BCZT ceramics prepared by solid state and sol-gel routes (see **Table. 5**). It is worth mentioning that the most important criteria that have to be considered during development of EC materials is the fact that the EC responsivity ($\Delta T/\Delta E$) should be as high as possible within a large interval of temperature [55]. The BCZT-4h exhibits a better EC responsivity with relatively large temperature interval ($FWHM_{\Delta T}$) of $\approx 33K$.

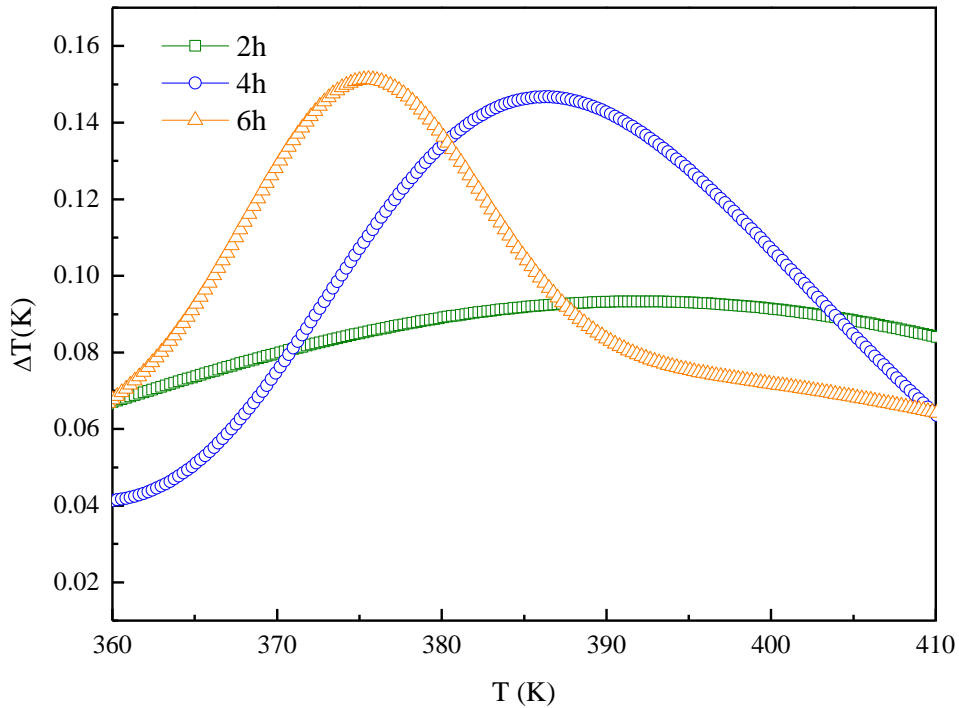


Fig. 11. Temperature profiles of the electrocaloric temperature change (ΔT) for various sintering times at 6 kV/cm applied electric field.

Table 5. Comparison of the ECE properties of BCZT ceramics with other lead-free materials reported in literature.

Material	Sintering regime (°C-h)	FWHM _{ΔT} (K)	ΔT _{EC,max} (K)	ΔE (kV/cm)	ξ (K mm/kV)	Synthesis method	Measurement method	Refs
Ba _{0.85} Ca _{0.15} Zr _{0.1} Ti _{0.9} O ₃ -2h	1420-2	56	0.0933	6	0.155	Sol-gel	Indirect	Present work
Ba _{0.85} Ca _{0.15} Zr _{0.1} Ti _{0.9} O ₃ -4h	1420-4	33	0.1467	6	0.244	Sol-gel	Indirect	Present work
Ba _{0.85} Ca _{0.15} Zr _{0.1} Ti _{0.9} O ₃ -6h	1420-6	23	0.1513	6	0.252	Sol-gel	Indirect	Present work
Ba _{0.85} Ca _{0.15} Zr _{0.1} Ti _{0.9} O ₃	1350-2	---	0.0150	6	0.025	Sol-gel	Indirect	[46]
Ba _{0.85} Ca _{0.15} Zr _{0.1} Ti _{0.9} O ₃	1420-2	---	0.1520	8	0.190	Solid state	Indirect	[56]
Ba _{0.8} Ca _{0.2} Zr _{0.06} Ti _{0.94} O ₃	1420-2	---	0.2100	7.95	0.264	Solid state	Indirect	[57]
0.65Ba(Zr _{0.2} Ti _{0.8})O ₃ -0.35(Ba _{0.7} Ca _{0.3})TiO ₃	1500-2	---	0.3300	20	0.165	Solid state	Direct	[58]
Ba _{0.98} Ca _{0.02} (Zr _{0.085} Ti _{0.915})O ₃	1280-2	---	0.6000	40	0.150	Solid state	Direct	[59]
Ba _{0.85} Ca _{0.15} Zr _{0.1} Ti _{0.9} O ₃	1400-4	---	0.4000	21.5	0.186	Solid state	Indirect	[60]
Ba _{0.8} Ca _{0.2} Zr _{0.04} Ti _{0.96} O ₃	1350-2	---	0.2700	7.95	0.340	Solid state	Indirect	[61]

4. Conclusion

In this contribution, we have dealt with the effect of sintering time on the structural, dielectric, ferroelectric and piezoelectric properties of lead-free Ba_{0.85}Ca_{0.15}Ti_{0.9}Zr_{0.1}O₃ (BCZT) ceramics prepared by sol-gel route. BCZT ceramic fabricated at 1420 °C for 4h with relative density of 98% has demonstrated simultaneously enhanced dielectric properties around the MPB region, i.e., $\epsilon_{r,max} = 16310$ and improved electrocaloric effect; $\zeta = 0.244$ K mm/kV. In addition, BCZT-4h displayed a relatively high Wrec of 10.61 mJ/cm³ with an efficiency coefficient of ~ 63% at low electric field strength. These results suggest that the synthesized BCZT-4h ceramic could be a promising candidate for electrocaloric and energy storage applications.

Acknowledgements

The authors gratefully acknowledge the financial support of the European H2020-MSCA-RISE-2017-ENGIMA action.

References

- [1] Z. Sun *et al.*, « Dielectric and piezoelectric properties and PTC behavior of Ba_{0.9}Ca_{0.1}Ti_{0.9}Zr_{0.1}O_{3-x}La ceramics prepared by hydrothermal method », *Mater. Lett.*, vol. 118, p. 1-4, mars 2014, doi: 10.1016/j.matlet.2013.12.043.
- [2] R. Bhimireddi, B. Ponraj, et K. B. R. Varma, « Structural, Optical, and Piezoelectric Response of Lead-Free Ba_{0.95}Mg_{0.05}Zr_{0.1}Ti_{0.9}O₃ Nanocrystalline Powder », *J. Am. Ceram. Soc.*, vol. 99, n° 3, p. 896-904, mars 2016, doi: 10.1111/jace.14018.
- [3] S. Sapatrya, T. Badapanda, S. Behera, B. Behera, et P. R. Das, « Effect of Gadolinium on the structural and dielectric properties of BCZT ceramics », *Phase Transit.*, vol. 93, n° 2, p. 245-262, févr. 2020, doi: 10.1080/01411594.2020.1711905.
- [4] S. D. Chavan et D. J. Salunkhe, « Ferroelectric Relaxation Behavior of Lead free BCZT Ceramics », vol. 3, n° 11, p. 5, 2012.
- [5] J. Tao, Z. Yi, Y. Liu, M. Zhang, et J. Zhai, « Dielectric Tunability, Dielectric Relaxation, and Impedance Spectroscopic Studies on (Ba_{0.85}Ca_{0.15})(Ti_{0.9}Zr_{0.1})O₃ Lead-Free Ceramics », *J. Am. Ceram. Soc.*, vol. 96, n° 6, p. 1847-1851, juin 2013, doi: 10.1111/jace.12265.
- [6] S. Ben Moumen *et al.*, « Impedance spectroscopy studies on lead free Ba_{1-x}Mg_x(Ti_{0.9}Zr_{0.1})O₃ ceramics », *Superlattices Microstruct.*, vol. 118, p. 45-54, juin 2018, doi: 10.1016/j.spmi.2018.04.012.
- [7] W. Cai *et al.*, « Synergistic effect of grain size and phase boundary on energy storage performance and electric properties of BCZT ceramics », *J. Mater. Sci. Mater. Electron.*, avr. 2020, doi: 10.1007/s10854-020-03446-z.
- [8] S. Ben Moumen *et al.*, « Structural, Dielectric, and Magnetic Properties of Multiferroic (Ba_{1-x}La_{0.5}Ca_{0.5}MnO₃)_{1-x}(BaTi_{0.8}Sn_{0.2}O₃)_x Laminated Composites », *IEEE Trans. Ultrason. Ferroelectr. Freq. Control*, vol. 66, n° 12, p. 1935-1941, déc. 2019, doi: 10.1109/TUFFC.2019.2935459.
- [9] P. Jaimeewong, M. Promsawat, A. Watcharapasorn, et S. Jiansirisomboon, « Comparative study of properties of BCZT ceramics prepared from conventional and sol-gel auto

- combustion powders », *Integr. Ferroelectr.*, vol. 175, n° 1, p. 25-32, oct. 2016, doi: 10.1080/10584587.2016.1199913.
- [10] J. Hao, W. Bai, W. Li, et J. Zhai, « Correlation Between the Microstructure and Electrical Properties in High-Performance (Ba_{0.85}Ca_{0.15})(Zr_{0.1}Ti_{0.9})O₃ Lead-Free Piezoelectric Ceramics », *J. Am. Ceram. Soc.*, vol. 95, n° 6, p. 1998-2006, juin 2012, doi: 10.1111/j.1551-2916.2012.05146.x.
- [11] N. Buatip *et al.*, « Investigation on electrical properties of BCZT ferroelectric ceramics prepared at various sintering conditions », *Integr. Ferroelectr.*, vol. 187, n° 1, p. 45-52, févr. 2018, doi: 10.1080/10584587.2018.1445395.
- [12] S.-W. Zhang, H. Zhang, B.-P. Zhang, et S. Yang, « Phase-transition behavior and piezoelectric properties of lead-free (Ba_{0.95}Ca_{0.05})(Ti_{1-x}Zr_x)O₃ ceramics », *J. Alloys Compd.*, vol. 506, n° 1, p. 131-135, sept. 2010, doi: 10.1016/j.jallcom.2010.06.157.
- [13] P. Yong, D. Shihua, N. Wenju, X. Qin, et W. Xiaoliang, « Dielectric Properties and Relaxor Behavior of Nd Doping BCZT Ceramics », *Ferroelectrics*, vol. 450, n° 1, p. 21-27, janv. 2013, doi: 10.1080/00150193.2013.838459.
- [14] Y. Tian, Y. Gong, D. Meng, H. Deng, et B. Kuang, « Low-temperature sintering and electric properties of BCT–BZT and BCZT lead-free ceramics », *J. Mater. Sci. Mater. Electron.*, vol. 26, n° 6, p. 3750-3756, juin 2015, doi: 10.1007/s10854-015-2898-2.
- [15] A. Thongtha, K. Angsukased, N. Riyamongkol, et T. Bongkarn, « Preparation of (Ba_{1-x}Sr_x)(Zr_xTi_{1-x})O₃ Ceramics via the Solid State Reaction Method », *Ferroelectrics*, vol. 403, n° 1, p. 68-75, oct. 2010, doi: 10.1080/00150191003748907.
- [16] M. Iranmanesh, M. Lingg, M. Stir, et J. Hulliger, « Sol gel and ceramic synthesis of Sr₂FeMo_{1-x}W_xO₆ (0 ≤ x ≤ 1) double perovskites series », *RSC Adv.*, vol. 6, n° 48, p. 42069-42075, 2016, doi: 10.1039/C6RA03923E.
- [17] M. Ito, M. Hagiwara, et S. Fujihara, « Hydrothermal synthesis of lead-free perovskite (Bi_{1/2}K_{1/2})(Zr_xTi_{1-x})O₃ powders », *J. Ceram. Soc. Jpn.*, vol. 125, n° 6, p. 454-457, 2017, doi: 10.2109/jcersj2.16263.
- [18] T. Kimijima, K. Kanie, M. Nakaya, et A. Muramatsu, « Solvothermal Synthesis of Shape-Controlled Perovskite MTiO₃ (M = Ba, Sr, and Ca) Particles in H₂O/Polyols Mixed Solutions », *Mater. Trans.*, vol. 55, n° 1, p. 147-153, 2014, doi: 10.2320/matertrans.M2013350.
- [19] Z. Wang *et al.*, « Synthesis, structure, dielectric, piezoelectric, and energy storage performance of (Ba_{0.85}Ca_{0.15})(Ti_{0.9}Zr_{0.1})O₃ ceramics prepared by different methods »,

- J. Mater. Sci. Mater. Electron.*, vol. 27, n° 5, p. 5047-5058, mai 2016, doi: 10.1007/s10854-016-4392-x.
- [20] Y. P. Jiang, X. G. Tang, S. G. Ju, Q. X. Liu, T. F. Zhang, et H. F. Xiong, « Influence of sintering temperature on the ferroelectric and piezoelectric properties of (Ba_{0.85}Ca_{0.15})(Zr_{0.1}Ti_{0.9})O₃ ceramics », *J. Mater. Sci. Mater. Electron.*, vol. 27, n° 3, p. 3048-3052, mars 2016, doi: 10.1007/s10854-015-4128-3.
- [21] J. Wu, D. Xiao, W. Wu, J. Zhu, et J. Wang, « Effect of dwell time during sintering on piezoelectric properties of (Ba_{0.85}Ca_{0.15})(Ti_{0.90}Zr_{0.10})O₃ lead-free ceramics », *J. Alloys Compd.*, vol. 509, n° 41, p. L359-L361, oct. 2011, doi: 10.1016/j.jallcom.2011.08.024.
- [22] W. Cai *et al.*, « Effects of oxygen partial pressure on the electrical properties and phase transitions in (Ba,Ca)(Ti,Zr)O₃ ceramics », *J. Mater. Sci.*, vol. 55, n° 23, p. 9972-9992, août 2020, doi: 10.1007/s10853-020-04771-8.
- [23] R. Liu, Y. Qiao, X. Zhang, et C.-X. Lu, « Effects of calcination temperatures on the morphology, architecture and dielectric properties of BCZT ceramics », *Bull. Mater. Sci.*, vol. 42, n° 4, p. 140, août 2019, doi: 10.1007/s12034-019-1825-1.
- [24] R. Liu, « Sol-gel Synthesis of (Ba_{0.85}Ca_{0.15})(Zr_{0.1}Ti_{0.9})O₃ Ceramics and their Dielectric Temperature Properties », p. 3.
- [25] Z. Hanani *et al.*, « Enhanced dielectric and electrocaloric properties in lead-free rod-like BCZT ceramics », *J. Adv. Ceram.*, vol. 9, n° 2, p. 210-219, avr. 2020, doi: 10.1007/s40145-020-0361-1.
- [26] S. Belkhadir *et al.*, « Impedance spectroscopy analysis of the diffuse phase transition in lead-free (Ba_{0.85}Ca_{0.15})(Zr_{0.1}Ti_{0.9})O₃ ceramic elaborated by sol-gel method », *Superlattices Microstruct.*, vol. 127, p. 71-79, mars 2019, doi: 10.1016/j.spmi.2018.03.009.
- [27] S. S. Mane et D. J. Salunkhe, « Structural and Dielectric Investigations on x[Ba_{0.7}Ca_{0.3}TiO₃]- $(1-x)$ [BaZr_{0.2}Ti_{0.8}O₃] Lead-Free Mixed Ceramic Compositions », vol. 4, n° 2, p. 6, 2013.
- [28] J. Wu, A. Habibul, X. Cheng, X. Wang, et B. Zhang, « Orthorhombic–tetragonal phase coexistence and piezoelectric behavior in $(1-x)$ (Ba,Ca)(Ti,Sn)O₃– x (Ba,Ca)(Ti,Zr)O₃ lead-free ceramics », *Mater. Res. Bull.*, vol. 48, n° 10, p. 4411-4414, oct. 2013, doi: 10.1016/j.materresbull.2013.06.035.
- [29] Ramovatar, I. Coondoo, S. Satapathy, N. Kumar, et N. Panwar, « Dielectric, Piezoelectric Enhancement and Photoluminescent Behavior in Low Temperature Sintered Pr-Modified Ba_{0.85}Ca_{0.15}Zr_{0.1}Ti_{0.9}O₃ Ceramics », *J. Electron. Mater.*, vol. 47, n° 10, p. 5870-5878, oct. 2018, doi: 10.1007/s11664-018-6472-6.

- [30] R. Jacob, H. G. Nair, et J. Isac, « Structural and Morphological Studies of Nanocrystalline Ceramic $\text{BaSr}_{0.9}\text{Fe}_{0.1}\text{TiO}_4$ », *Int. Lett. Chem. Phys. Astron.*, vol. 41, p. 100-117, nov. 2014, doi: 10.18052/www.scipress.com/ILCPA.41.100.
- [31] X. Ji *et al.*, « Structural and electrical properties of BCZT ceramics synthesized by sol-gel-hydrothermal process at low temperature », *J. Mater. Sci. Mater. Electron.*, vol. 30, n° 13, p. 12197-12203, juill. 2019, doi: 10.1007/s10854-019-01578-5.
- [32] A. Mirzaei, M. Bonyani, et S. Torkian, « Synthesis and characterization of nanocrystalline PZT powders: From sol to dense ceramics », *Process. Appl. Ceram.*, vol. 10, n° 1, p. 9-16, 2016, doi: 10.2298/PAC1601009M.
- [33] P. Parjansri, U. Intatha, K. Pengpat, et S. Eitssayeam, « Improvement in the electrical properties of BCZT Ceramics induced by self-seeds », *Appl. Phys. A*, vol. 125, n° 6, p. 421, juin 2019, doi: 10.1007/s00339-019-2711-9.
- [34] Y. Tian, Y. Gong, Z. Zhang, et D. Meng, « Phase evolutions and electric properties of BaTiO_3 ceramics by a low-temperature sintering process », *J. Mater. Sci. Mater. Electron.*, vol. 25, n° 12, p. 5467-5474, déc. 2014, doi: 10.1007/s10854-014-2330-3.
- [35] Ch. Rayssi, S. El.Kossi, J. Dhahri, et K. Khirouni, « Frequency and temperature-dependence of dielectric permittivity and electric modulus studies of the solid solution $\text{Ca}_{0.85}\text{Er}_{0.1}\text{Ti}_{1-x}\text{Co}_{4x/3}\text{O}_3$ ($0 \leq x \leq 0.1$) », *RSC Adv.*, vol. 8, n° 31, p. 17139-17150, 2018, doi: 10.1039/C8RA00794B.
- [36] S. Mitra, A. R. Kulkarni, et O. Prakash, « Diffuse phase transition and electrical properties of lead-free piezoelectric $(\text{Li}_x\text{Na}_{1-x})\text{NbO}_3$ ($0.04 \leq x \leq 0.20$) ceramics near morphotropic phase boundary », *J. Appl. Phys.*, vol. 114, n° 6, p. 064106, août 2013, doi: 10.1063/1.4817815.
- [37] P. Bharathi et K. B. R. Varma, « Grain and the concomitant ferroelectric domain size dependent physical properties of $\text{Ba}_{0.85}\text{Ca}_{0.15}\text{Zr}_{0.1}\text{Ti}_{0.9}\text{O}_3$ ceramics fabricated using powders derived from oxalate precursor route », *J. Appl. Phys.*, vol. 116, n° 16, p. 164107, oct. 2014, doi: 10.1063/1.4900494.
- [38] R. Yevych, M. Medulych, et Y. Vysochanskii, « Nonlinear dynamics of ferroelectrics with three-well local potential », *Condens. Matter Phys.*, vol. 21, n° 2, p. 23001, juin 2018, doi: 10.5488/CMP.21.23001.
- [39] S. Hunpratub, S. Maensiri, et P. Chindapasirt, « Synthesis and characterization of $\text{Ba}_{0.85}\text{Ca}_{0.15}\text{Ti}_{0.9}\text{Zr}_{0.1}\text{O}_3$ ceramics by hydrothermal method », *Ceram. Int.*, vol. 40, n° 8, p. 13025-13031, sept. 2014, doi: 10.1016/j.ceramint.2014.04.166.

- [40] I. Coondoo, N. Panwar, H. Amorín, M. Alguero, et A. L. Kholkin, « Synthesis and characterization of lead-free $0.5\text{Ba}(\text{Zr}_{0.2}\text{Ti}_{0.8})\text{O}_3-0.5(\text{Ba}_{0.7}\text{Ca}_{0.3})\text{TiO}_3$ ceramic », *J. Appl. Phys.*, vol. 113, n° 21, p. 214107, juin 2013, doi: 10.1063/1.4808338.
- [41] A. Belboukhari *et al.*, « Studies of Diffuse Phase Transition in Ferroelectric Solid Solution $\text{Pb}_{1-x}\text{K}_{2x}\text{Nb}_2\text{O}_6$ ($x = 0.1, 0.2, 0.25$ and 0.3) », *Ferroelectrics*, vol. 444, n° 1, p. 116-124, janv. 2013, doi: 10.1080/00150193.2013.786619.
- [42] M. Q. Awan, J. Ahmad, L. Norén, T. Lu, et Y. Liu, « Structure, dielectric and ferroelectric properties of lead free $(\text{K,Na})(\text{Nb})\text{O}_3-x\text{BiErO}_3$ piezoelectric ceramics », *J. Mater. Sci. Mater. Electron.*, vol. 29, n° 9, p. 7142-7151, mai 2018, doi: 10.1007/s10854-018-8702-3.
- [43] W. Janbua, T. Bongkarn, T. Kolodiaznyi, et N. Vittayakorn, « High piezoelectric response and polymorphic phase region in the lead-free piezoelectric $\text{BaTiO}_3-\text{CaTiO}_3-\text{BaSnO}_3$ ternary system », *RSC Adv.*, vol. 7, n° 48, p. 30166-30176, 2017, doi: 10.1039/C7RA04017B.
- [44] A. Khesro *et al.*, « Temperature Dependent Piezoelectric Properties of Lead-Free $(1-x)\text{K}_0.6\text{Na}_0.4\text{NbO}_3-x\text{BiFeO}_3$ Ceramics », *Front. Mater.*, vol. 7, p. 140, mai 2020, doi: 10.3389/fmats.2020.00140.
- [45] X. Ji *et al.*, « Structural and electrical properties of BCZT ceramics synthesized by sol-gel process », *J. Mater. Sci. Mater. Electron.*, vol. 29, n° 9, p. 7592-7599, mai 2018, doi: 10.1007/s10854-018-8751-7.
- [46] S. Belkhadir *et al.*, « Structural, dielectric and electrocaloric properties of $(\text{Ba}_{0.85}\text{Ca}_{0.15})(\text{Ti}_{0.9}\text{Zr}_{0.1-x}\text{Sn}_x)\text{O}_3$ ceramics elaborated by sol-gel method », *J. Mater. Sci. Mater. Electron.*, vol. 30, n° 15, p. 14099-14111, août 2019, doi: 10.1007/s10854-019-01776-1.
- [47] P. Kantha *et al.*, « Effect of Sintering Method on the Microstructure and Dielectric Properties of Lead-Free BCZT Ceramics », *Appl. Mech. Mater.*, vol. 866, p. 263-266, juin 2017, doi: 10.4028/www.scientific.net/AMM.866.263.
- [48] I. Coondoo *et al.*, « A comparative study of structural and electrical properties in lead-free BCZT ceramics: Influence of the synthesis method », *Acta Mater.*, vol. 155, p. 331-342, août 2018, doi: 10.1016/j.actamat.2018.05.029.
- [49] H. Yang, F. Yan, Y. Lin, et T. Wang, « Novel Strontium Titanate-Based Lead-Free Ceramics for High-Energy Storage Applications », *ACS Sustain. Chem. Eng.*, vol. 5, n° 11, p. 10215-10222, nov. 2017, doi: 10.1021/acssuschemeng.7b02203.

- [50] V. S. Puli *et al.*, « Structure, dielectric, ferroelectric, and energy density properties of $(1-x)\text{BZT}-x\text{BCT}$ ceramic capacitors for energy storage applications », *J. Mater. Sci.*, vol. 48, n° 5, p. 2151-2157, mars 2013, doi: 10.1007/s10853-012-6990-1.
- [51] X. Chen, X. Chao, et Z. Yang, « Submicron barium calcium zirconium titanate ceramic for energy storage synthesised via the co-precipitation method », *Mater. Res. Bull.*, vol. 111, p. 259-266, mars 2019, doi: 10.1016/j.materresbull.2018.11.025.
- [52] D. Zhan, Q. Xu, D.-P. Huang, H.-X. Liu, W. Chen, et F. Zhang, « Dielectric nonlinearity and electric breakdown behaviors of $\text{Ba}_{0.95}\text{Ca}_{0.05}\text{Zr}_{0.3}\text{Ti}_{0.7}\text{O}_3$ ceramics for energy storage utilizations », *J. Alloys Compd.*, vol. 682, p. 594-600, oct. 2016, doi: 10.1016/j.jallcom.2016.04.317.
- [53] A. Bauzá, T. J. Mooibroek, et A. Frontera, « Towards design strategies for anion- π interactions in crystal engineering », *CrystEngComm*, vol. 18, n° 1, p. 10-23, 2016, doi: 10.1039/C5CE01813G.
- [54] D. Li et S.-G. Lu, « Electrocaloric Effect and Phase Transitions in Ferroelectrics », *Int. J. Metall. Mater. Eng.*, vol. 4, n° 1, avr. 2018, doi: 10.15344/2455-2372/2018/141.
- [55] H. Kaddoussi, A. Lahmar, Y. Gagou, J.-L. Dellis, H. Khemakhem, et M. E. Marssi, « Electro-caloric effect in lead-free ferroelectric $\text{Ba}_{1-x}\text{Ca}_x(\text{Zr}_{0.1}\text{Ti}_{0.9})_{0.925}\text{Sn}_{0.075}\text{O}_3$ ceramics », *Ceram. Int.*, vol. 41, n° 10, p. 15103-15110, déc. 2015, doi: 10.1016/j.ceramint.2015.08.080.
- [56] H. Kaddoussi *et al.*, « Sequence of structural transitions and electrocaloric properties in $(\text{Ba}_{1-x}\text{Ca}_x)(\text{Zr}_{0.1}\text{Ti}_{0.9})\text{O}_3$ ceramics », *J. Alloys Compd.*, vol. 713, p. 164-179, août 2017, doi: 10.1016/j.jallcom.2017.04.148.
- [57] G. Singh, V. S. Tiwari, et P. K. Gupta, « Electro-caloric effect in $(\text{Ba}_{1-x}\text{Ca}_x)(\text{Zr}_{0.05}\text{Ti}_{0.95})\text{O}_3$: A lead-free ferroelectric material », *Appl. Phys. Lett.*, vol. 103, n° 20, p. 202903, nov. 2013, doi: 10.1063/1.4829635.
- [58] M. Sanlialp, V. V. Shvartsman, M. Acosta, B. Dkhil, et D. C. Lupascu, « Strong electrocaloric effect in lead-free $0.65\text{Ba}(\text{Zr}_{0.2}\text{Ti}_{0.8})\text{O}_3-0.35(\text{Ba}_{0.7}\text{Ca}_{0.3})\text{TiO}_3$ ceramics obtained by direct measurements », *Appl. Phys. Lett.*, vol. 106, n° 6, p. 062901, févr. 2015, doi: 10.1063/1.4907774.
- [59] J. Wang, T. Yang, S. Chen, G. Li, Q. Zhang, et X. Yao, « Nonadiabatic direct measurement electrocaloric effect in lead-free $\text{Ba,Ca}(\text{Zr,Ti})\text{O}_3$ ceramics », *J. Alloys Compd.*, vol. 550, p. 561-563, févr. 2013, doi: 10.1016/j.jallcom.2012.10.144.

- [60] S. Patel, A. Chauhan, et R. Vaish, « Enhanced electrocaloric effect in Fe-doped (Ba_{0.85}Ca_{0.15}Zr_{0.1}Ti_{0.9})O₃ ferroelectric ceramics », *Appl. Mater. Today*, vol. 1, n° 1, p. 37-44, nov. 2015, doi: 10.1016/j.apmt.2015.08.002.
- [61] B. Asbani *et al.*, « Lead-free Ba_{0.8}Ca_{0.2}(Zr_xTi_{1-x})O₃ ceramics with large electrocaloric effect », *Appl. Phys. Lett.*, vol. 106, n° 4, p. 042902, janv. 2015, doi: 10.1063/1.4906864.